2022-01-0967 Published 15 Jun 2022

ANC: A Low-Cost Implementation Perspective

Costante Belicchi and Alessandro Opinto University of Parma

Marco Martalo University of Cagliari

Anna Tira, Daniel Pinardi, Angelo Farina, and Gianluigi Ferrari University of Parma

Citation: Belicchi, C., Opinto, A., Martalo, M., Tira, A. et al., "ANC: A Low-Cost Implementation Perspective," SAE Technical Paper 2022-01-0967, 2022, doi:10.4271/2022-01-0967.

Received: 07 Dec 2021 Revised: 28 Mar 2022 Accepted: 29 Mar 2022

Abstract

In the present work, we describe a low-cost implementation of an Active Noise Cancellation (ANC) system. The most interesting feature of our implementation is the use of general-purpose hardware, without the need of expensive and hard-to-program Digital Signal Processing (DSP) devices. In particular, the reference signals, collected with accelerometers properly placed on noise-generating parts and the error feedback signals are collected by means of an USB interface. All signal processing, aimed at primary path estimation and anti-noise audio signal generation, is performed using Simulink running on a commercial mini PC. The Exponential Sine Sweep (ESS) method is adopted for the measurement of the secondary path from the cancellation loudspeakers to the error microphones. An adaptive Filtered-X Least Mean Square (LMS) algorithm determines the anti-noise audio signal to be emitted. The system has been installed and tested on a commercial agricultural tractor cabin mounted over electromagnetic shakers to emulate realistic operating conditions. Two error microphones are attached to the headrest, close to the driver's ears. The resulting ANC system relies on the use of very small buffers (for audio/accelerometric data), with a latency comparable to that of more complex and expensive specific DSP systems used in this kind of applications. In terms of acoustic performance, a significant reduction of annoying peaks in the 200-500 Hz range and a broadband noise reduction at lower frequencies are observed, thus improving the overall sound quality experience. In conclusion, the implementation of an effective ANC system, employing common audio devices and a relatively simple Simulink program, was obtained. This paves the way to straightforward experimentation (in Matlab/Simulink) of new ANC processing algorithms, allowing direct testing of simulation-based solutions, without the need of porting them to a proprietary DSP-based platform.

Introduction

As part of the solutions aimed at improving comfort and safety on board agricultural tractors with cabs, by reducing the driver's exposure to disturbing acoustic waves, traditional passive mitigation methods, which involve the use of sound-absorbing and sound-insulating materials, may be not very effective in controlling low-frequency components. Within the car cabins and, mostly, the cabs of agricultural machinery, the noise at the driver's ear is characterized by low- and medium-frequency components deriving from sources such as the engine or road-tire interaction [1]. Since the late 1980s, studies on Active Noise Control (ANC) systems, mentioned for the first time in a patent from 1936 [2], for noise mitigation within car cabin have been carried out by Elliot et al [3]. Inspired by these results in the automotive field, ANC studies have been then carried out in the field of tractors and other agricultural machinery [4]. From a technical point of view, the ANC method is based on the emission, through a dedicated loudspeaker, of an acoustic signal, usually referred to as anti-noise, of equal amplitude and opposite phase with respect to the disturbing audio wave. Ideally, these two audio signals destructively overlaps each other obtaining perfect silence in the point of space where they are incident. In reality, noise cancellation is limited by hardware delays and physical constraints. Moreover, a perfect noise cancellation is unfeasible due to hardware and software components limits. In most of the commercial solutions and studies in the literature, dedicated, complex and expensive Digital Signal Processing (DSP) devices have been employed in order to effectively implement real-time ANC systems. The aim of this work is to implement a FeedForward (FF) Single Input-Single Output (SISO) ANC system with cross-channels compensation by using general-proposed hardware devices. In order to reduce prototyping times, we opted for a system based on devices that could easily integrate a Windows operating system and the Matlab/Simulink software with which the ANC system was developed. Two electromagnetic shakers, installed in the left and right front tractor cabin, emit dedicated audio signals to vibrate the cabin structure simulating realistic mechanical vibrations. Microphone, reference and anti-noise signals are managed by a professional audio interface. The developed ANC system was aimed at acting on the structure-borne component of the noise in the cabin and a Filtered-x Least Mean Square (FxLMS)

control algorithm has been employed for its operation. The estimation of the Secondary Path (SP), implemented in Simulink, has been performed by using the Exponential Sine Sweep (ESS) method [5]. Our results show that a good trade-off between system performance and material costs is obtained thanks to a smart solution with down-and up-sampling of the signals performed by Simulink software. Appreciable noise reductions are achieved by both error microphones when periodic disturbance signals, typical of a tractor cabin environment, are considered. Moreover, our prototype showed limited, but robust cancellation, also for realistic disturbance signals. For this reason, our proposed solution can be considered as valid for testing ANC systems by avoiding expensive software and hardware. This paper is structured as follows. In the first part of the article, the hardware components used are described in detail. Mathematical backgrounds on the FxLMS algorithm for the control of the considered ANC system is illustrated. Subsequently, the Matlab/Simulink models implemented for the estimation of SP is described. Finally, the experimental results are presented.

Experimental Setup

In this section, the ANC system experimental setup is presented. First, the hardware and physical equipment are considered. Then, the FxLMS algorithm and the secondary paths estimation method are discussed.

Hardware and Equipment

This section describes the various devices which compose the developed ANC prototypical system, with the aim of installing the system on the tractor cab. Starting from the controller, the device of choice had to support a Windows operating system and to have good computational capabilities with limited costs and dimensions. A solution based on an Intel NUC mini PC [6] was adopted, as they meet the required specifications. The system selected to carry out the first tests is the Intel NUC8i7BEH NUC, equipped with an Intel CoreTM i7-8559U processor with 32 GB of RAM (DDR4 SO-DIMM sockets) and 1 TB of SSD disk. The tests demonstrated the computational capabilities needed to run the Simulink models underlying the ANC system. However, NUC mini PCs have reduced audio processing performance. To this end, the controller has been equipped, via USB connection, with an external RME Fireface UCX [7] audio interface. The chosen model also allows, by means of an equalizer that can be set from the software control panel, a filtering of the input/output signals. Assigning part of the necessary signal filtering to the audio interface allows one to lighten the computational load of Simulink models by reducing the latencies of the control system. The audio interface is meant to acquire the error and reference signals as input and to emit the anti-noise signals as output. The device has 8 outputs and 8 inputs, of which only two are equipped with 48 V phantom power. In order to acquire more than two signals from ICP sensors, which all require an external power supply, an external amplification device has been connected to the RME UCX inputs without phantom power. In order to avoid problems of power supply and excessive bulk, when installed on the tractor cab, the choice fell on a small electronic board, developed at the University of Parma specifically for the purpose of providing phantom power to up to three ICP sensors. This board can be powered simply by a small battery, from 18 V to 30 V, which provides a stable CC power supply. The acoustic emission of the antinoise signal for cancellation was entrusted to two 140 mm loudspeakers chosen for their dynamic behavior at medium-low frequencies, that is the range where the ANC system mainly acts. They were installed in the cabin positioned rear of the driver's head. This position was chosen because it was considered a good compromise between the operational performance of the ANC system and the use of the space in the tractor cab. To power the two speakers it was necessary to use a power amplifier: the choice fell on the JVC car model KS-DR3004 [8]. The system tests were carried out on a cabin previously disassembled from a real vehicle. In order to stress this cabin, it was installed on supports equipped with electromagnetic shakers, through which vibration signals of different nature could be applied to the structure. The considered shakers are depicted in Figure 1(a and b) for the left and right front sides, respectively. The goal was to cause an overall vibration of the cabin, through the stress of the shakers, simulating the real mechanical components of the tractor. This vibration causes the acoustic noise in the cabin that the designed ANC system has to reduce. As shown in Figure 1, the accelerometers, highlighted by red circles, have been installed near the stress positions of the cabin. These accelerometers were used to provide the reference signals for the ANC system. With the aim of absorbing part of the reflected acoustic waves, a manikin has been positioned at the driver's position. Two error microphones have been installed around the noise cancellation is desired, i.e., at the left and right driver's ears. More precisely, the distance between manikin's ears and microphones is about 30 cm. For this work, two 1/2 inch omnidirectional ICP microphones for free-field measurements with a sensitivity of 31.6 mV/Pa by Brüel&Kjær, have been employed. The loudspeakers dedicated for the anti-noise emissions have been placed close to the manikin's head in order to improve

FIGURE 1 Shakers and accelerometers installation at the tractor cabin structure. (a) left front side, (b) right front side.

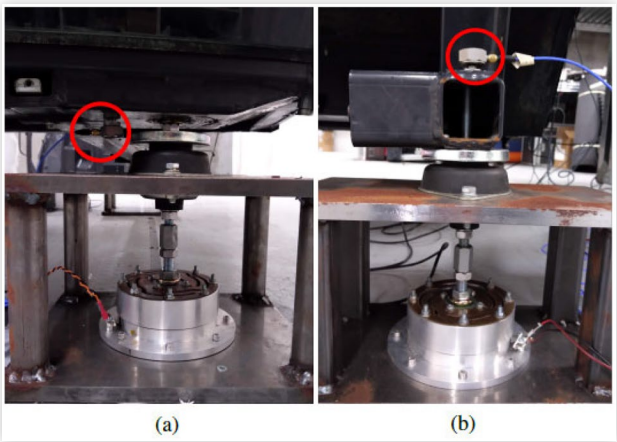

FIGURE 2 Experimental setup and measurements equipment: error microphones, loudspeakers for anti-noises emission and manikin at the driver's position.

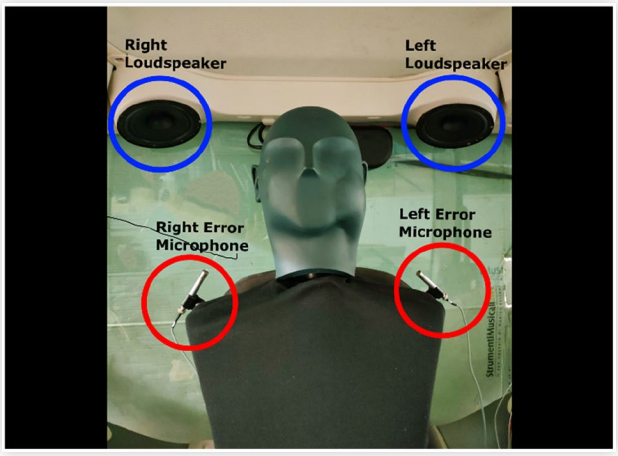

the noise cancellation performance thanks to the reduced microphone/loudspeaker distance (about 34cm). The considered setup described above is depicted in Figure 2.

FxLMS Algorithm

The discrete-time block diagram of a FF multiple reference parallel SISO ANC system with cross-channel compensation based on FxLMS algorithm is shown in Figure 3. The block P(z), usually referred to as primary path, represent the physical channels between the J reference signals and the M error microphone. The disturbing signal detected by the m-th transducer can thus be expressed as

$$d_m[n]=\sum_{j=1}^{J}x_j[n]\otimes p_{jm}[n] \tag{1}$$

where $x_j[n]$ and $p_{jm}[n]$ identify the j-th reference signal and primary path impulse response associated to the m-th microphone, respectively, and $\otimes$ denotes the convolution operator. The acoustic channels between the loudspeakers for the anti-noises emission and the microphones are called secondary paths and, in the frequency domain, can be represented by a set of Finite Impulse Response (FIR) filters $S(z)$. From Figure 3, at the output of the set of adaptive filters$\mathbf{W}(z)$, the k-th anti-noise signal can be written as

$$y_k[n]=\sum_{j=1}^{J}\mathbf{x}_j^{\mathrm{T}}[n]\mathbf{w}_{jk}[n] \tag{2}$$

where the j-th reference vector and the control filter tap-weight vector between the j-th reference signal and the k-th loudspeaker at the n-th time epoch are respectively defined as

$$\mathbf{x}_j[n]=\left[x_j[n],x_j[n-1],\ldots,x_j[n-N+1]\right]^{\mathrm{T}} \tag{3}$$

$$\mathbf{w}_{jk}[n]=\left[w_{jk0}[n],w_{jk1}[n],\ldots,w_{jk,N-1}[n]\right]^{\mathrm{T}} \tag{4}$$

being N the control filter length and Tthe transpose operator. At the m-th error microphone, a sum of the anti-noises contributions filtered by the corresponding acoustic channel is obtained, i.e.,

$$y'_m[n]=\sum_{k=1}^{K}y_k[n]\otimes s_{mk}[n] \tag{5}$$

where $s_{mk}[n]$ is the impulse response of $S_{mk}(z)$ associated to the m-th error microphone and the k-th loudspeaker. Finally, at the m-th error microphone, the acoustic sum of the disturbing audio signal $d_m[n]$ and its opposite phase version $y'_m[n]$ is obtained. Mathematically, the error signal $e_m[n]$ is

$$e_m[n]=d_m[n]+y'_m[n]=d_m[n]+\sum_{k=1}^{K}y_k[n]\otimes s_{mk}[n]. \tag{6}$$

FIGURE 3 Discrete-time block diagram of a FF multiple reference parallel SISO ANC system with cross-channel compensation based on FxLMS algorithm.

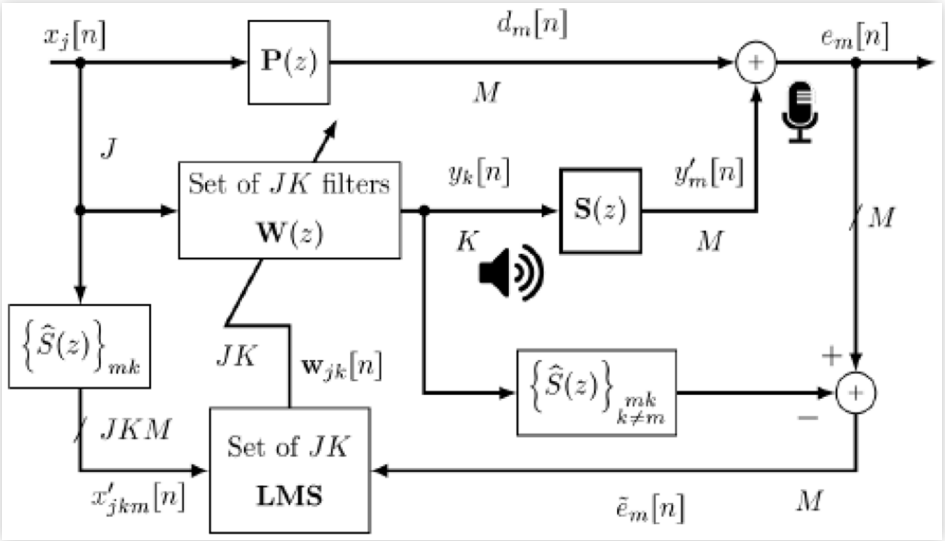

The purpose of LMS algorithm is to estimate the control filter tap-weights in order to minimize the cost function $\xi[n]$ [9]. In this scenario, the relevant error signal to be minimized with respect to the filter tap-weights is defined as the sum of the error signals coming from the M error microphones, i.e., the Multiple Input-Multiple Output (MIMO) approach. Another possible solution is to use this system as a parallel SISO, i.e., left and right anti-noise loudspeakers employed to minimized corresponding left and right error microphone. However, when ANC system is contemporaneously ON by both sides, each error microphone perceives both the direct and the cross anti-noise. In this case, channel interference of the secondary paths may significantly deteriorate the system performance. To cope with this issue, a new error signal $\tilde{e}_m[n]$ can be defined as

$$\tilde{e}_m[n] = e_m[n] - \sum_{\substack{k=1 \\ k \neq m}}^{K} y_k[n] \otimes s_{mk}[n]. \tag{7}$$

Hence, for the M error microphones, it is possible to calculate the cost function separately, i.e., $\xi_m[n] = \tilde{e}_m[n]$. Its gradient can be evaluated as follows

$$\begin{aligned} &\frac{\partial \xi_m[n]}{\partial w_{jki}} = \frac{\partial \tilde{e}_m^2[n]}{\partial w_{jki}} = 2\tilde{e}_m[n]\frac{\partial \tilde{e}_m[n]}{\partial w_{jki}} = \\ &= 2\tilde{e}_m[n]\left(s_{mk}[n] \otimes x_j[n-i]\right) = \\ &= 2\tilde{e}_m[n]x'_{jkm}[n-i] \end{aligned} \tag{8}$$

where, it has been assumed a perfect secondary paths estimation, i.e., $\hat{S}(z) = S(z)$. By defining

$$\mathrm{x}'_{jkm}[n] = [\hat{s}_{mk}[n] \otimes x_j[n], \ldots, \hat{s}_{mk}[n] \otimes x_j[n-N+1]]^{\mathrm{T}} \tag{9}$$

it is possible to compactly write

$$\nabla \xi_m[n] = 2\tilde{e}_m[n]\mathrm{x}'_{jkm}[n] \tag{10}$$

Recalling that the update recursion of the steepest descent algorithm for the m-th microphone is

$$\mathbf{w}_{jk}[n+1] = \mathbf{w}_{jk}[n] - \frac{1}{2}\mu \nabla \xi_m[n] \tag{11}$$

and substituting (10) into (11), the recursive tap-weights equation associated to j-th reference signal and the k-th loudspeaker for the leaky normalized LMS algorithm is

$$\mathbf{w}_{jk}[n+1] = \lambda \mathbf{w}_{jk}[n] - \mu \frac{\mathrm{x}'_{jkm}[n]}{\varepsilon + \mathrm{x}'^{\mathrm{T}}_{jkm}[n]\mathrm{x}'_{jkm}[n]}\tilde{e}_m[n] \tag{12}$$

where λ is the so-called leakage factor and controls the algorithm memory, μ is the step-size parameter which adjusts the convergence speed and ε is a positive constant introduced in order to prevent computational precision error when the normalization factor $\mathbf{x}'^{\mathrm{T}}_{jkm}[n]\mathbf{x}'_{jkm}[n]$ is too small [10].

Secondary Path Analysis

The goal of this work was to develop a low-cost ANC system by using hardware easily available and software with sensible ease of use. Hence, dedicated MATLAB and Simulink-based applications have been developed to perform the signal processing for the noise cancellation. As previously mentioned, in an ANC system, the secondary path (SP) represents the transfer function between the loudspeaker for the anti-noise emission and the error microphone. Thus, the SP provides information on the transformations that the cabin environment applies to the anti-noise signal emitted before being perceived by the error microphone in the cancellation position. Moreover, the SP has a significant impact on system performance. In the literature, several adaptive algorithms have been proposed for SP estimation, e.g., by employing LMS algorithm with white noise as input and reference signal [11]. In our prototype, the SPs have been estimated by employing the Exponential Sine Sweep (ESS) method. The rationale behind this algorithm is to play, from the loudspeakers used for the anti-noises emission, a known signal $x(t)$, i.e., the exponential sine sweep audio wave, and to record, by the error microphones, the received audio signal $r(t)$. Hence, after evaluating the so-called inverse filter $x^{-1}(t)$, it is possible to retrieve the considered secondary path by convolving $r(t)$ with the inverse signal. In Figure 4(a and b), the exponential sine sweep signal $x(t)$ and the inverse filter $x^{-1}(t)$ is shown, respectively. The block diagram of the considered SP estimation method is depicted in Figure 5. In order to compensate with the unknown delay introduced by the buffer, electronics and computing, the so-called loop-back connections have been implemented in the audio interface. In other words, the sine sweep audio wave played by the audio interface and at the output of the loudspeaker, is fed-back with a jack connection to input microphones. Thus, the loop-back signal $l(t)$ can be compared with the received one and the correct fly-time between loudspeakers and microphones can be estimated. With the aim of shaping the secondary path response, the signals, i.e., $r(t)$, $x^{-1}(t)$ and $l(t)$, are band-limited within 0-500 Hz by employing an Infinite Impulse Response (IIR) filter $G(f)$.

FIGURE 4 Exponential sine sweep (a) and inverse filter (b) as a function of time.

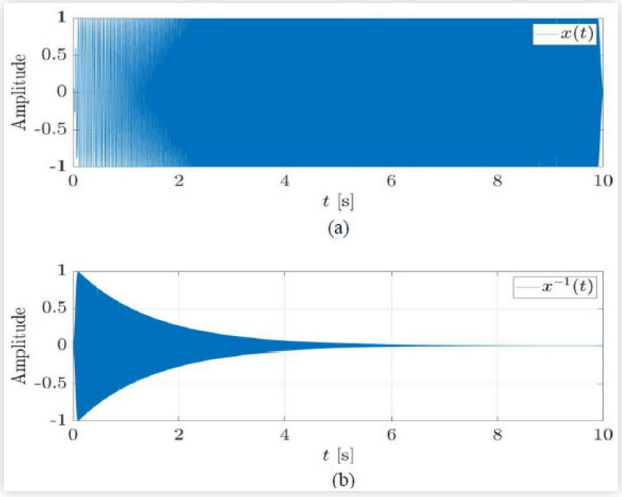

FIGURE 5 Block diagram of secondary path estimation.

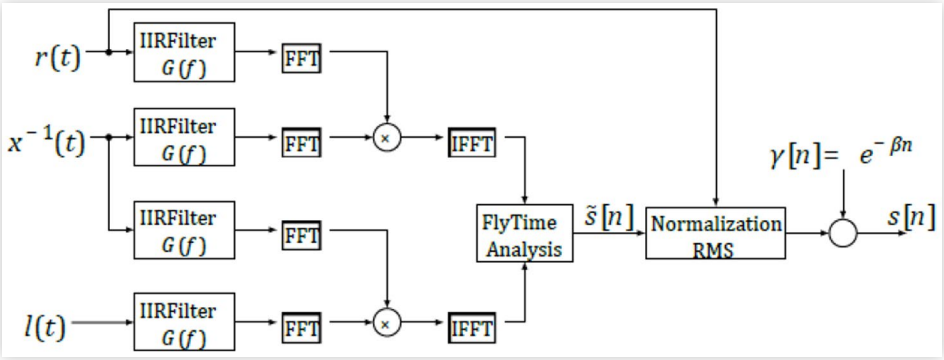

In our prototype, the SP length has been set to 8192 samples and a sine sweep of duration 10 seconds has been used. In particular, the sampling frequency f_s = of 32 kHz and a buffer size of 2048 samples have been set in the audio interface. After passing through the FFT and IFFT blocks that perform the Fast Fourier Transform (FFT) and Inverse Fast Fourier Transform (IFFT), the preliminary estimation of the secondary path Impulse Response (IR) $\tilde{s}[n]$ is obtained. Then, the impulse response is normalized with respect to the Root Mean Square (RMS) of the input signal $r(t)$ and, in order to reduce the computational complexity, it is truncated up to the first $N_{cut} = f_s/10 = 3200$ samples. Finally, the IR $\tilde{s}[n]$ is weighted by using the following exponential function

$$\gamma[n] = e^{-\beta n} \tag{13}$$

where n is the discrete-time and β is a scalar number set in such a way to have $\gamma[N_{cut}] \leq 10^{-2}$. The final IR $s[n]$ is thus given by

$$s[n] = \gamma[n] \odot \tilde{s}[n] \tag{14}$$

where $\odot$ denotes the element-wise multiplication operator. Note that, the goal of the weighting function in (13) is to obtain a smoother IR shape and to give less weight to the tails. This signal processing improves the system performance since that the delay associated to the secondary paths is reduced. As an example, in Figure 6, the magnitude response of the SP between the left loudspeaker (number 1) and the left error microphone (number 1), i.e., $|S_{11}(f)|$ is shown. It is possible to easily observe that this filter is band-limited within 600 Hz thanks to the introduction of filter $G(f)$ and equalization specification performed by the audio interface RME side. Moreover, note that very low-frequency contributions are also limited.

FIGURE 6 Magnitude response of the secondary path between left loudspeaker and left error microphone 1 $|S_{11}(f)|$.

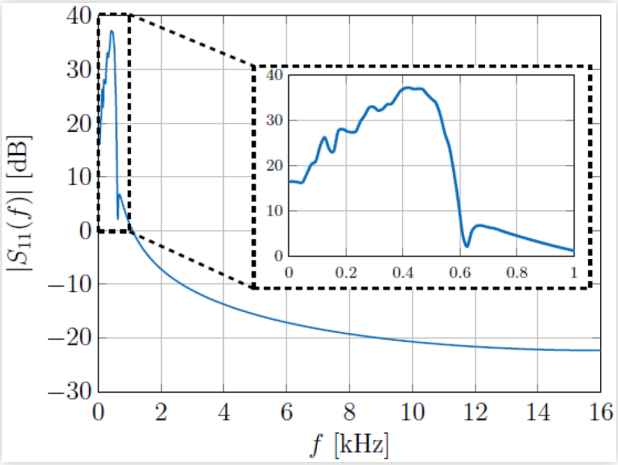

Experimental Results

In this section the experimental results of FF multiple reference parallel SISO adaptive ANC system with cross-channels compensation are presented. The parameters of the FxLMS algorithm, i.e., the leakage-factor λ and step-size μ in (12) have been empirically set in order to maximize noise cancellation performance. A control filter length of $N = 1024$ samples has been set. As previously mentioned, the sample rate f_s of the audio interface RME has been set to 32 kHz. However, signal processing performed at high-frequency induce to computational overload by the pc and latency problems. For this reason, once reference and microphone signals are acquired by the RME, they are down-sampled at the Simulink level by a factor $K_{factor} = 8$, yielding thus a sample-rate $F_S = 4$ kHz. Of course, in order to not incur into aliasing issues a low-pass filter (LPF) with a cut-off frequency $f_c = 600$ Hz is employed before the down-sampling operation. Hence, signals with a sample-rate of F_S are processed by the adopted FxLMS algorithm in order to evaluate the anti-noise signals $y_1[n]$ and $y_2[n]$. This means that also the SPs, discussed in the previous Section, are down-sampled by the K_{factor}, yielding thus to a SP filter length of 400 samples, corresponding to an impulse response duration of 100 ms. Similarly to what has been performed at the input level, anti-noise signals are up-sampled by K_{factor} and filtered by the LPF. Finally, the anti-noise signals feed the audio interface RME and they are emitted by the loudspeakers. The block diagram of the interface between adopted hardware/equipment and the NUC PC/software is depicted in Figure 7 where also the loudspeakers, microphones and secondary paths are shown. The noise cancellation performance is assessed in terms of microphone signal evolution against time and Sound Pressure Level (SPL) when the ANC system is OFF and ON. The SPL or acoustic pressure level is a measurement of the effective sound pressure of a mechanical wave with

FIGURE 7 Block diagram between hardware/equipment and NUC PC/software.

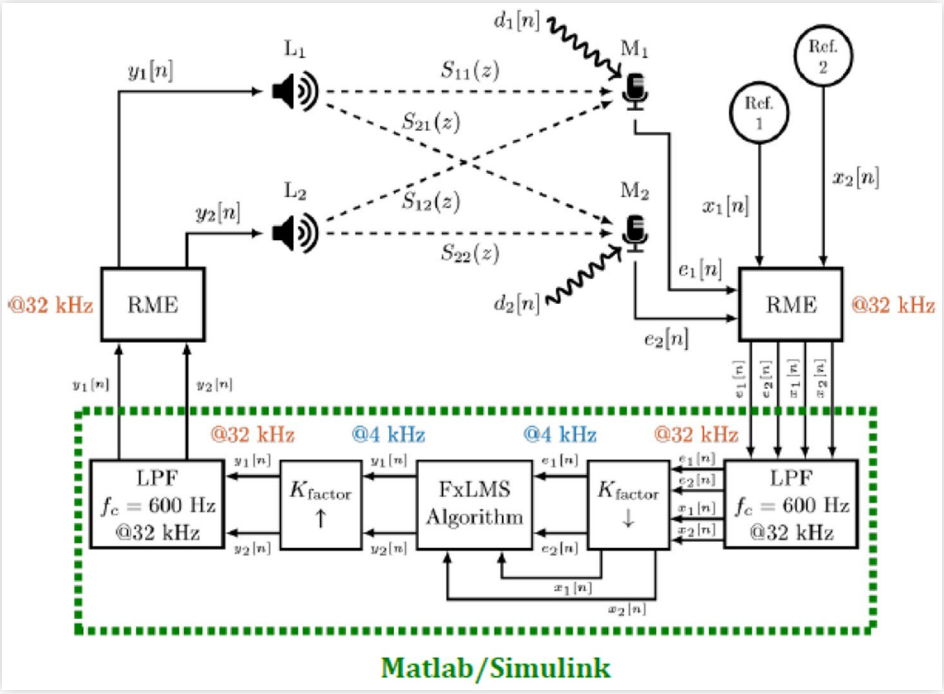

respect to a reference sound source. A logarithmic measure of the SPL spectrum is defined as

$$s(f) = 20\log_{10}\left(\frac{p(f)}{p_0}\right) \tag{15}$$

where $p(f)$ is the sound pressure in a specific Resolution Bandwidth (RBW) centered at a frequency f, measured in μPa and p_0 is the reference sound pressure, conventionally set to 20μPa for air. In our prototype, the RBW has been set to 6 Hz. Moreover, in order to take into account to the relative loudness perceived by the human ear, the microphone signals are filtered by the A-weighting filter [12, 13]. Hence the dimension of the SPL spectrum is [dBA/Hz].

Unlike the disturbing signals perceived by the microphones within a car that are usually dominated by almost broad-band low-frequency regime, within a tractor cabin a more tonal signals are exhibited [4, 14]. For this reason, as a representative of realistic vibrations, a sinusoidal signal at a fundamental frequency f_d = 300 Hz has been used to feed the shakers and excite the tractor cabin. The corresponding results for parallel SISO ANC system with cross-channel compensation are presented in Figures 8 and 9 for the left and right error microphone, respectively. In particular, sub-figures (a) depict the microphone signal evolution as a function of time and sub-figures (b) show the SPL as a function of the frequency when the ANC system is OFF an ON.

The ANC system starts in OFF mode and after a small period of time it is turned ON. By observing the microphone signals evolution, in Figure 8(a) and Figure 9(a), it is possible to note that, initially, the ANC system is not effective: this is because the FxLMS algorithm convergence is not yet achieved. In fact, both microphones exhibit significant noise reduction after about 50 seconds. By comparing the two microphone

FIGURE 8 Results for tractor cabin excited by a pure tone at f_d = 300 Hz. Left error microphone signal evolution against time (a) and SPL spectra (b) when ANC system is OFF and ON .

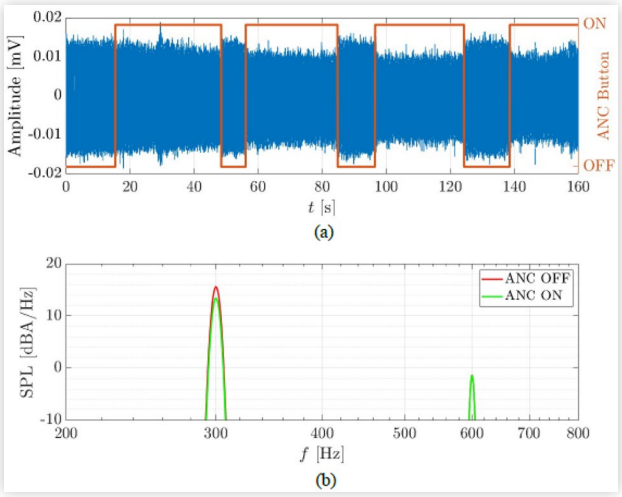

signals evolution, one can notice that an higher level of sound is perceived by the right microphone with respect to the left one and the disturbing audio signal is better mitigated. This can be confirmed by observing the corresponding SPL spectra for both microphones in Figs. 8(b) and 9(b). The SPL of the right error microphone is higher than the left one and a noise cancellation up to 4.5 dB is exhibited at the considered tonal input at f_d = 300 Hz. Note that the ANC system cannot attenuate the second harmonic at 600 Hz, because of (i) the low-pass filtering of the SPs and (ii) the considerably small energetic level perceived by the microphones with respect to the fundamental one. In order to test the ANC system robustness under

FIGURE 9 Results for tractor cabin excited by a pure tone at f_d = 300 Hz. Right error microphone signal evolution against time (a) and SPL spectra (b) when ANC system is OFF and ON.

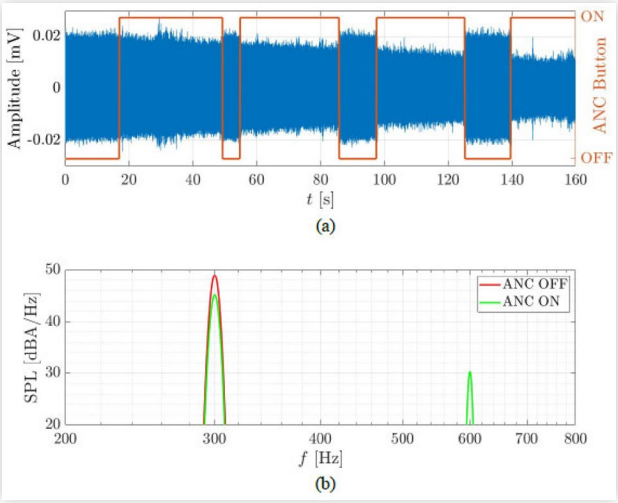

different scenarios and input signal type, two sinusoidal audio waves centered at f_{d1} = 260 Hz and f_{d2} = 440 Hz have been employed to vibrate the cabin. Experimental results, in terms of SPL spectra, for the left and right error microphone are shown in Figure 10(a) and Figure 10(b), respectively. Both error microphones nicely mitigate the disturbance signals. In general, the left error microphone exhibits better performance with the right one. Especially for f_{d2}, one can notice a noise cancellation level that up to 5 dB and 2 dB is obtained for the left and right error microphone, respectively. Unfortunately, the ANC system is not significantly effective for the pure tone centered at *fd*1. In fact, both error microphones show a maximum noise reduction of about 1.5 dB at a frequency of 260 Hz. This may be due to the fact that, at this specific

FIGURE 10 Results for tractor cabin excited by two pure tones at f_{d_1} = 260 Hz and f_{d_2} = 440 Hz. SPL spectra when ANC system is OFF and ON for left (a) and right (b) error microphone.

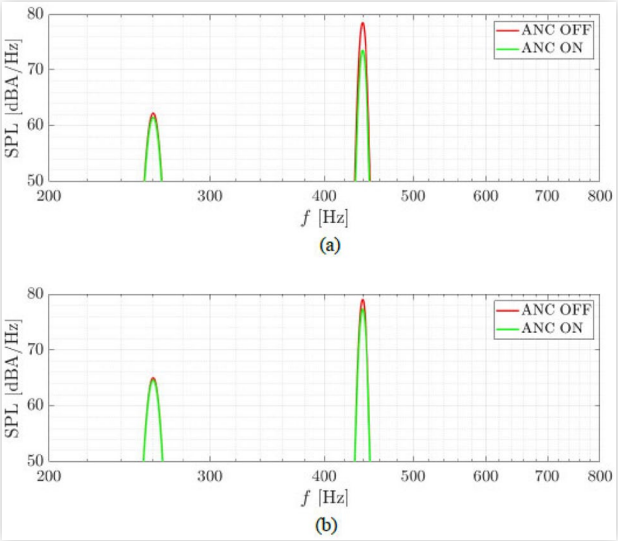

FIGURE 11 Results for tractor cabin excited by realistic environmental noise. One third octave band when ANC system is OFF and ON for left error microphone.

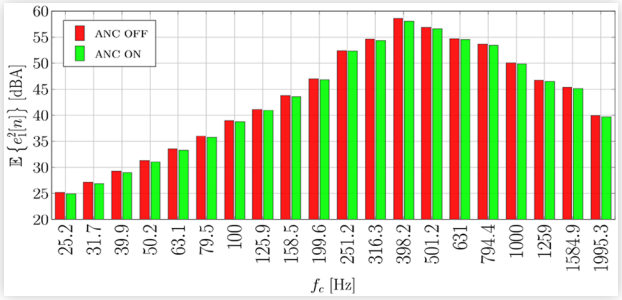

frequency, the SPs exhibits a low-gain and also by the lower energy level of the microphone signal compared to that experienced at 440 Hz.

Finally, an experimental measurement of environmental sound propagating within the cabin of a tractor moving at a speed of 40 km/h has been used to shake the cabin and thus testing the ANC system under a realistic scenario. In this case, the experimental results are discussed in terms of mean square of the m-th error signal $\tilde{e}_m^2[n]$ when the ANC system is OFF and ON, i.e.,

$$\mathbb{E}\left\{\tilde{e}_m^2[n][n]\right\} = \frac{1}{N}\sum_{n=0}^{N-1}\tilde{e}_m^2[n] \tag{16}$$

Where $\mathbb{E}$ denotes the expected operator, N is the considered window length (in terms of number of samples) for the mean square evaluation. In particular, for visualization convenience, since realistic microphone signals experience several and rapid oscillations, this performance indicator has been evaluated as a function of the frequency band, i.e., the error microphone signal in (16) has been decomposed into 1/3 octave-bands. For the sake of compactness, only the left error microphone is considered. The corresponding results are shown in Fig.11, where f_c denotes the central frequency of the considered sub-band filter. As expected, due to time-varying nature and the presence of broad-band frequency contributions of the disturbance signal, ANC system performance degrades. However, it is possible to note that, for the whole bandwidth, no amplification effects are obtained. On the other hand, for the mid-frequency range, small noise mitigation can be appreciated, e.g., within 199.6-501.2 Hz. Similar considerations ca be drawn also for the right error microphone.

Conclusions

In this paper, a low-cost and practical ANC system implementation for realistic agricultural machinery has been presented. A multiple reference parallel adaptive SISO ANC system with cross-channel compensation based on FxLMS algorithm has been developed by using Matlab/Simulink software on an Intel NUC mini PC. The RME Fireface UCX audio interface, with a sample rate of 32 kHz, has been employed to acquire microphone and reference signals. In order to reduce the

computational delay caused by a high sampling frequency, at Simulink level proper signal processing with down-sampling (followed by up-sampling to generate emitted audio signal) is performed. SPs have been estimated with the ESS method by using a Simulink-based software. Experimental results show that our ANC prototype is able to nicely mitigate disturbance signals with periodic behavior at different frequencies. System performance degrades when realistic time-varying disturbance signals are considered. However, no noise amplification occurs within the whole frequency band and slight small noise cancellations are obtained under realistic and stressful conditions. Therefore, our prototype can be considered as an efficient solution to the considered ANC problem, since it guarantees good performance at a very low materials cost.

List of Abbreviations

ANC - Active Noise Cancellation or Control;
ESS - Exponential Sine Sweep;
FF - Feedforward;
FxLMS - Filtered-x Least Mean Square;
IR - Impulse Response;
LMS - Least Mean Square;
LPF - Low-Pass Filter;
MIMO - Multiple Input-Multiple Output;
RBW - Resolution Bandwidth.
SISO - Single Input-Single Output;
SP - Secondary Path;
SPL - Sound Pressure Level;

References

1. Abd-El-Tawwab, A.M., Abouel-Seoud, S., El-Sayed, F., and Abd-El-Hakim, T., "Characteristics of Agriculture Tractor Interior Noise," *Journal of Low Frequency Noise, Vibration and Active Control* 19, no. 2 (2000): 73-81, doi:10.1260/0263092001492822.
2. Lueg, P., Process of silencing sound oscillations. US Patent 2,043,416, June 9, 1936.
3. Elliott, S., Stothers, I., Nelson, P., McDonald, A. et al., "The Active Control of Engine Noise Inside Cars," Presented at in *INTER-NOISE and NOISE-CON 1988*, 987-990, 1988.
4. Gulyas, K., Pinte, G., Augusztinovicz, F., Desmet W. et al., "Active Noise Control in Agricultural Machines," in *Proceedings of the ISMA 2002*, Belgium, September 2002.
5. Farina, A., "Simultaneous Measurement of Impulse Response and Distortion with a Swept-Sine Technique," *Journal of the Audio Engineering Society* (2000).
6. Intel, "Intel NUC," accessed November 2021, www.intel.com/content/www/us/en/products/boards-kits/nuc.html.
7. RME Audio, "RME Fireface UCX Audio Interface," accessed November 2021, www.rme-audio.de/fireface-ucx.html.
8. JVC, "JVC KS-DR3004 Power Amplifier," accessed November 2021, eu.jvc.com/mobile-entertainment/amplifiers/KSDR3004/.
9. Boroujeny, B.F., *Adaptive Filters: Theory and Applications*, 2nd ed. (New York: John Wiley & Sons, 2013).
10. Hayes, M.H., *Statistical Digital Signal Processing and Modeling*, 1st ed. (New York: John Wiley & Sons, 1996).
11. Opinto, A., Martalò, M., Tripodi, C., Costalunga, A. et al, "Performance Analysis of Feedback MIMO ANC in Experimental Automotive Environment," in *2020 14th International Conference on Signal Processing and Communication Systems (ICSPCS)*, 1-6, 2020, doi:10.1109/ICSPCS50536.2020.9310039.
12. Bies, D.A. and Hansen, C.H., *Engineering Noise Control: Theory and Practice*, 4th ed. (CRC Press, 2009).
13. Thompson, A., and Taylor, B.N., "Guide for the Use of the International System of Units (SI)," National Institute of Standard and Technology, Special Publication 811, 2008, doi:10.6028/NIST.SP.811e2008.
14. Nelson, A. and Elliott, S.J., *Active Control of Sound* (New York: Academic Press, 1991).

Contact Information

Costante Belicchi
Department of Engineering and Architecture
University of Parma, Italy
e-mail address: costante.belicchi@unipr.it

ISSN 0148-7191